1 # Multivariate pattern analysis of fMRI data for imaginary and real

2 # colours in grapheme-colour synaesthesia

3

4

5 **Running title**

6 MVPA of grapheme-colour synaesthesia

7

8

9 **Mathieu J. Ruiz** (1,2), **Michel Dojat** (2), **Jean-Michel Hupé** (1)

10 (1) Centre de Recherche Cerveau et Cognition, Université de Toulouse Paul Sabatier & CNRS, 31300

11 Toulouse, France

12 (2) Grenoble Institut des Neurosciences, Université Grenoble Alpes, INSERM & CHU Grenoble Alpes,

13 38000 Grenoble, France

14

15

21   **Abstract**

22   Grapheme-colour synaesthesia is a subjective phenomenon related to perception and imagination, in

23   which some people involuntarily but systematically associate specific, idiosyncratic colours to

24   achromatic letters or digits. Its investigation is relevant to unravel the neural correlates of colour

25   perception in isolation from low-level neural processing of spectral components, as well as the neural

26   correlates of imagination by being able to reliably trigger imaginary colour experiences. However,

27   functional MRI studies using univariate analyses failed to provide univocal evidence of the activation

28   of the 'colour network' by synaesthesia. Applying Multivariate (multivoxel) Pattern Analysis (MVPA)

29   on 20 synaesthetes and 20 control participants, we tested whether the neural processing of real

30   colours (concentric rings) and synaesthetic colours (black graphemes) shared patterns of activations.

31   Region of interest analyses in retinotopically and anatomically defined visual regions revealed neither

32   evidence of shared circuits for real and synaesthetic colour processing, nor processing difference

33   between synaesthetes and controls. We also found no correlation with individual experiences,

34   characterised by measuring the strength of synaesthetic associations. The whole brain, searchlight,

35   analysis led to similar results. We conclude that identifying the neural correlates of the synaesthetic

36   experience of colours may still be beyond the reach of present technology and data analysis

37   techniques.

38

2

41   **Introduction**

42   Synaesthesia is a subjective experience shared by only a fraction of the population (Simner et al.,

43   2006; Chun & Hupé, 2013; Simner & Carmichael, 2015; Rouw & Scholte, 2016; Watson et al., 2017),

44   offering, in principle, an opportunity to study the neural bases of subjective experience, drawing on

45   individual differences just like in neuropsychology, but involving healthy people. Moreover, colour,

46   the typical prototype of a qualia (what it feels like to perceive something) is the most often cited (or

47   at least studied: Ward, 2013) content of the synaesthetic experience. However, the very subjective

48   nature of the synaesthetic experience represents a major obstacle when trying to set an objective

49   and operational definition, as required in an experimental protocol. Not only subjective descriptions

50   may vary a lot between subjects (Flournoy, 1893), but also within subjects when asked to complete

51   the same questionnaire again (Edquist, Rich, Brinkman, & Mattingley, 2006) or when describing their

52   subjective experience of colour for different letters (Hupé, Bordier, & Dojat, 2012b). Using

53   psychophysical tests, the synaesthetic experience of colour appears more similar to imagined or

54   remembered than perceived colours (Witthoft & Winawer, 2013; Chiou & Rich, 2014; Hupé & Dojat,

55   2015; Janik McErlean & Banissy, 2017). The experience of synaesthetic colours can be indeed

56   formally described as a form of mental imagery, since it occurs without any corresponding spectral

57   stimulation. The obligatory experience of colour when exposed to letters or digits may therefore

58   justify the label of 'intrusive visual imagery' (Reeder, 2016). Unfortunately, this simplification does

59   not help much with defining the phenomenological content of synaesthesia, since self-reports of

60   mental imagery show at least as much diversity as those of synaesthesia (Galton, 1880), with mixed

61   evidence about whether the presence of synaesthesia may relate to individual differences in mental

62   imagery (Chun & Hupé, 2016). One may, however, study how much synaesthesia requires the neural

63   resources involved in visual perception. This bottom-up approach, which does not address the

64   phenomenological issue, can at least be operationalized. Moreover, grapheme-colour synaesthesia

65   offers a unique opportunity regarding the neural correlates of imagination as it restrains both

66   individual variability and the content specificity of visual imagery. Last but not least, synaesthetic

67   colours are systematically triggered by letters and digits, unlike "regular" mental imagery that

68   depends on both the good will and the (uneven) ability of subjects.

69   Several brain imaging studies have compared activations in the visual cortex for real and synaesthetic

70   colours, whose majority did not reveal any overlap. There were even questions whether activations

71   triggered by synaesthetic stimuli, when observed, were in fact related to the synaesthetic experience

72   at all (Hupé & Dojat, 2015). This surprising 'Null' result may be due to methodological limitations

73   since only massive univariate analysis of brain imaging data were used so far, which may reveal only

74   processes well localized in the brain (Hupé et al., 2012b). Multivariate (multivoxel) Pattern Analysis

75   (MVPA) does not suffer from such a restriction. MVPA provides a way to reveal how information is

76   encoded by the brain (Cox & Savoy, 2003; Norman, Polyn, Detre, & Haxby, 2006; Formisano &

77   Kriegeskorte, 2012; Hebart & Baker, 2017). It has been applied successfully to the decoding of

78   aspects of mental images (Thirion et al., 2006; Reddy, Tsuchiya, & Serre, 2010). Using fMRI, here we

79   simply asked whether classifiers trained on patterns of blood oxygenation dependent signals (BOLD

80   responses) elicited by different coloured stimuli could predict which synaesthetic colours were

81   experienced by synaesthetes when seeing achromatic letters and digits. We studied in particular the

82   early stages of visual processing by identifying cortical areas V1 to V4 in each subject, using

83   retinotopic mapping, thus avoiding the problems related to structural normalization (Poldrack, 2007;

84   Hupé, 2015). We also explored the whole visual cortex (including parts of the parietal cortex) using

85   regions of interest based on a probabilistic atlas (Eickhoff et al., 2007), and performed whole brain

86   searchlight analyses (Kriegeskorte, Goebel, & Bandettini, 2006). We compared all the measures

87   obtained in synaesthetes with those obtained in a group of non-synaesthetes to take into account

88   any potential non-specific effect related to the choice of stimuli. We also took into account the

89   individual variability of the synaesthetic experience: without any possibility to characterize

90   objectively the different phenomenological accounts, we measured the strength of the synaesthetic

91   associations (Ruiz & Hupé, 2015).

92

93   **Materials and Methods**

94   **Participants**

95   We tested 20 synaesthetes and 20 non-synaesthetes. Synaesthetes (17 women) were between 21

96   and 42 years old (M = 27.9, SD = 5.5). Recruitment was diverse and opportunistic, based on self-

97   referral following publicity on internet: lab webpage, *Facebook* event, announcements on university

98   networks in Grenoble and Paris. Potential participants, after a first phone interview, were asked by

99   email to fill-up a questionnaire to describe their synaesthetic associations and for grapheme colour

100   associations to send us a list of those. Synaesthetes were included if they had a sufficient and diverse

101   number of letter-colour and digit-colour associations as required by the design of our experiments

102   (see below). When they came to the laboratory to perform the experiments, they had a semi-

103   directed interview to evaluate the phenomenology of their synesthetic associations. They also ran a

104   modified version of the "Synaesthesia Battery Test" (Eagleman, Kagan, Nelson, Sagaram, & Sarma,

105   2007) to choose precisely the colour of each letter and digit. This procedure was also used as a retest

106   to confirm the validity of the first-person reports (Ruiz & Hupé, 2015): in all subjects, all chosen

107   colours matched those indicated by print or by name in the questionnaire. In addition, objective

4

108   measurements of synaesthetic associations were obtained by Stroop-like tests (see below in the
109   'Protocol' section). Seven of the included synaesthetes had already participated in psychophysics
110   experiments between 2007 and 2010 (Ruiz & Hupé, 2015).

111   Control participants were recruited after synaesthetes to match their demographic statistics (16
112   women, age range between 23 and 38 years old, M = 28.5, SD = 4.3), following similar advertisement
113   strategies as well as soliciting colleagues at the Grenoble Institute of Neuroscience. Interviews were
114   conducted to verify the absence of any type of synaesthesia, not only the absence of grapheme-
115   colour associations. We chose not to run any consistency score with the control subjects in order not
116   to prime them to do any voluntary association between graphemes and colours before the tests in
117   the scanner. It could be argued that some of the controls may have had implicit synaesthetic
118   associations they were not aware of, as it sometimes happens. In any case, this unlikely possibility
119   could not bias our results because most of our analyses did not require any direct comparison of the
120   performances by synaesthetes and controls.

121   The study was performed in accordance with the Declaration of Helsinki, it received approval by the
122   Institutional Review Board of Grenoble (CPP 12-CHUG-17, approval date 04/04/2012) and written,
123   informed consent was obtained from all subjects. A medical doctor verified that all subjects were
124   without past or current brain disease and had no detected cognitive deficit. All subjects had normal
125   colour perception on the Lanthony D-15 desaturated colour test (Richmond products), and normal or
126   corrected to normal eyesight (then using MRI-compatible glasses).

127   **Materials**

128   Stimuli: for each synaesthete, we tried to identify four pairs of graphemes made of one letter and
129   one digit that had similar colour associations. We never chose graphemes for which a synaesthete
130   indicated several colours. We tried to find pairs of red, green, blue and yellow (R, G, B, Y) graphemes,
131   but we were only partially successful and in some cases we selected a pair from the most saturated
132   colours available. Figure 1 shows the actual letters and digits with colours used in the experiments.
133   Only 13 subjects named the pairs red, green, blue and yellow; other colours were named orange,
134   violet, fuchsia and brown, as well as light and dark blue or green. Syn08 and syn48 had a pair made of
135   two letters. Since each synaesthete was tested with a different set of stimuli, each control subject
136   was tested with the stimuli of a specific synaesthete (with the exception of syn10 who had no
137   matched control, by mistake; two controls were tested instead with the stimuli of syn11. Paired
138   comparisons were therefore based on 38 subjects).

139
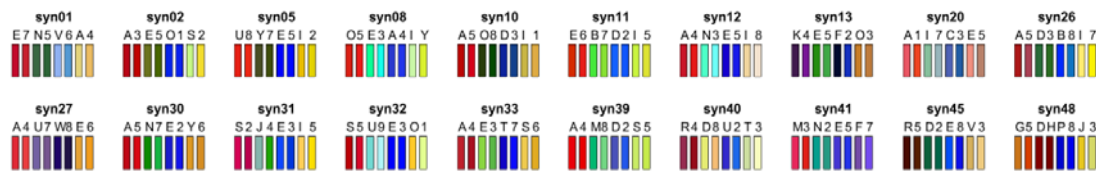
Figure 1. Letters and digits used for each synaesthete, with their corresponding synaesthetic RGB colours (the rendering of the colours using the projector in the scanner was different).

In the MR scanner, we presented these letters and digits in black at the centre of the screen (upper case, Helvetica font, extent up to 2 degrees eccentricity) over a grey uniform background (CIE xyY [0.29 0.3 77.4], half of the maximal luminance of the screen). Stimuli were projected on a translucent screen at the back of the scanner by a video projector Epson EMP 8200. We used a spectrophotometer (PhotoResearch PR 650) for colour and luminance measurements used to compute calibrated images. We also presented dynamic concentric rings (square luminance profile, similar to the stimuli used by Brouwer & Heeger, 2009, except for the absence of anti-aliasing so as to use only the colours selected by each synaesthete), with the exact same (real) colours as those chosen by each synaesthete for each grapheme. The choice of colours matching the individual grapheme 'R, G, B, Y' colour associations was done again by each synaesthete in the scanner over the same grey background, using a house-modified MRI compatible, comfortable, 10-button console controller, and the colour-picker of the "Synaesthesia Battery Test" as was done previously outside of the scanner. The same coloured rings were used for each matched control. The rings extent was also up to 2 degree eccentricity and the spatial frequency was 3 cycles/degree (six circles). The phase of the rings changed randomly at 6 Hz to almost nullify visual effects induced by the absence of anti-aliasing.

These stimuli were chosen with the purpose of training and testing classifiers (see below, "Data analysis: classifications"). Briefly, we wanted to use the BOLD responses to the coloured rings to train classifiers on colours, and the BOLD responses to graphemes to train classifiers on synaesthetic colours. This required choosing pairs of dissimilar graphemes, i.e. a letter and a digit, to try to avoid that the classifier trained on some shared form features, but rather on their common associated colour. This also implied that decoding should not be feasible that way based on the responses of control subjects. The use of pairs of graphemes also allowed the training on letters and testing on digits (or the reverse), with success in principle possible only for synaesthetes, based on their synaesthetic colour associations. The careful matching procedure of synaesthetic colours allowed the training of classifiers on real colours and testing on graphemes to identify which brain regions, if any,

170   coded both real and synaesthetic colours. Again, any decoding success would in principle be possible

171   only in synaesthetes.

172   Classifiers would be trained and tested on four categories, 'R, G, B, and Y', referring either to the real

173   or the synaesthetic prototypical colours that we tried to select. To maximize classification

174   performances, categories should be perceptually disjoint. Figure 2 represents the actual colours used

175   in the scanner for each synaesthete within the CIE L*a*b* colour space, which is more perceptually

176   uniform than the CIE xyY space. As was already obvious in Figure 1, differences of luminance were

177   important to distinguish stimuli. Figure 2 illustrates that the colour and luminance distances were not

178   similar across subjects between categories and within pairs, leading to unequal clusterisation. We

179   could even expect some confusions by the classifiers for some subjects (e.g. "green/yellow" for

180   syn11, "red/blue" for syn13 or "blue/yellow" for syn41). While the maximal theoretical performance

181   achievable by classifiers was therefore below 100%, classifiers could however obtain more than the

182   25% chance performance in every subject. For all the analyses (described below), we tested if the

183   performance of classifiers across subjects was correlated with the ratio of colour distance (indicated

184   for each subject in Table 1) as measured in the L*a*b* space; we did not find any evidence of that,

185   except for the classification of colours in the searchlight analysis, when testing the group of

186   synaesthetes: we found one significant cluster (106 voxels, 2862 mm^3), in the left fusiform gyrus,

187   peaking at MNI XYZ = [-27 -73 -4], extending from about V4 to FG4, in line with the involvement of

188   these regions in colour processing.
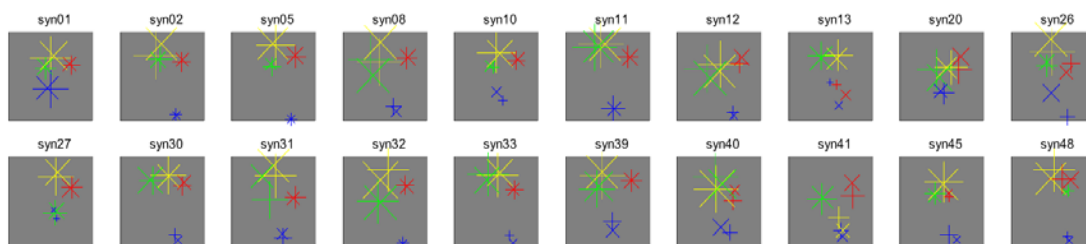
189
190   **Figure 2.** Colour coordinates in the CIE L*a*b* space of the stimuli used for each synaesthete, corresponding to the

191   idiosyncratic synaesthetic colours of letters (+) and digits (x). The colours of the crosses are arbitrary and correspond to the

192   four categories the classifiers had to distinguish. The size of the crosses is proportional to luminance (marker size = 0.4*L,

193   where max(L) = 100; axes limits are +/- 130, possible range being −128 to +127).

194

195   Note that luminance variations constitute a major difference, due to the constraint of using

196   synaesthetic colours, with other MVPA studies of the neural correlates of colour processing, which

197   used isoluminant stimuli (Brouwer & Heeger, 2009; Parkes, Marsman, Oxley, Goulermas, & Wuerger,

198   2009). We do not know how differences along the luminance axis should be perceptually scaled to

199   differences along the green/red opponent colours a* axis and the blue/yellow opponent colours b*

200 axis. This question is probably an ill-posed problem when studying brain correlates of colour

201 perception, since at the cortical level visual circuits rely on both (but with different degrees) the

202 parvo- and the magno-cellular pathways (Tootell & Nasr, 2017).

203 **Protocol**

204 Each subject ran three fMRI sessions of about 1 hour. In addition, synaesthetes ran a 1 hour

205 psychophysics experiment (before or interleaved with fMRI experiments, depending on schedule

206 availability) to measure the strength of their synaesthetic associations using variants of Stroop tasks.

207 All the details of the psychophysics experiment as well as the results of 11 synaesthetes are

208 published (Ruiz & Hupé, 2015). Briefly, eight graphemes (repeated 36 times each) were presented

209 randomly either with the colour chosen by each synaesthete (congruent condition) or with the

210 synaesthetic colour of the other presented graphemes (incongruent condition). Synaesthete had to

211 name as fast as possible the real colour of the grapheme ('colour' task). Response times were

212 measured *a posteriori* based on the audio recording. The procedure was then repeated, but

213 synaesthetes had this time to name as fast of possible the name of the synaesthetic colour (called a

214 photism) they associated to each grapheme, which was also either congruent or incongruent with

215 the real colour of the stimulus ('photism' task). The index of the strength of synaesthetic associations

216 ('photism strength') combined two measures: the response time difference for congruent and

217 incongruent stimuli in the colour task, which reflects the difficulty to inhibit synaesthetic

218 associations; the response time difference to name the real and the synaesthetic colours (in the

219 congruent condition), which reflects how easily synaesthetes retrieve the synaesthetic colour.

220 The data of one synaesthete (syn40) could not be analysed because the chosen orange and

221 yellow/green colours revealed too similar (see Figure 2) and were not named consistently over the

222 course of the experiment. Table I provides a summary of the data. It shows that even synaesthetes

223 who obtained a relatively low score of photism strength (e.g., syn01) were very fast at naming the

224 synaesthetic colour of letters and numbers, even though the real colour of the stimulus was

225 systematically varied. Moreover, they very rarely made any mistake (Ruiz & Hupé, 2015). Such a task

226 would be extremely difficult to perform by any non-synaesthete trying to memorize (without

227 training) random colour associations. These data therefore provide a further objective validation of

228 the genuineness of the synaesthetic experience of these participants as well as an estimate of the

229 strength of the associations.

230

231

					Colour			Photism		
					Congruent	Incongruent	Congruency effect	Congruent	Incongruent	Photism delay
Synaesthete	Age	Sex	Distance ratio	**Photism strength**	CC	CI	CI-CC	PC	PI	PC-CC
syn01	21	F	13	**-107**	443	454	12	561	685	119
syn02	21	F	13	**52**	466	543	77	491	543	25
syn05	30	F	38	**20**	452	501	49	480	568	29
syn08	35	M	6	**69**	484	585	101	516	619	32
syn10	31	F	9	**40**	556	633	77	593	689	37
syn11	28	F	21	**146**	643	782	138	636	681	-7
syn12	33	F	9	**136**	597	683	86	548	646	-50
syn13	29	F	4	**30**	668	744	76	714	795	46
syn20	23	F	4	**19**	506	556	50	537	637	31
syn26	27	M	4	**-19**	497	528	31	547	690	50
syn27	24	F	10	**-4**	547	582	36	586	676	39
syn30	27	F	14	**416**	466	844	378	427	449	-39
syn31	24	F	6	**20**	525	573	47	553	639	27
syn32	33	F	12	**-57**	456	477	21	534	620	78
syn33	30	F	11	**-30**	447	457	10	487	525	40
syn39	26	F	13	**48**	440	523	83	475	582	35
syn40	42	F	5	**NaN**						
syn41	23	F	6	**-15**	484	514	30	529	678	45
syn45	27	F	10	**10**	539	564	25	554	691	16
syn48	22	M	9	**-73**	487	529	42	602	770	115

232

233 **Table 1**. Demographics and characteristics of the tested synaesthetes. The variable 'Distance ratio' is a measure of
234 clusterisation of the pairs of colour (average between-cluster distance divided by average within-cluster distance, measured
235 in the L*a*b* space). The higher the value, the better the clusterisation (see Figure 2). The variable 'Photism strength' is the
236 measure of the strength of synaesthetic associations as developed by Ruiz et al. (2015), based on the results of Stroop like
237 tests. The next columns indicate the median time measured in *ms* for each subject to name either the real ('Colour') or the
238 synaesthetic colour ('Photism') of the letters and numbers shown in Figure 1, when the real colour was either congruent or
239 incongruent with the synaesthetic colour indicated by each synaesthete. The 'Congruency effect' was measured as the
240 difference of response time in the 'Colour' condition. 'Photism delay' is the difference between naming the real and the
241 synaesthetic colours, and 'Photism strength' is the difference of these two values. The interpretation of this index is only
242 relative (the zero value does not have any special meaning). The data of syn40 data were not consistent (see text).

243

244   **fMRI experiments**

245   The MR experiments were performed at the IRMaGe MRI facility (Grenoble, France) with a 3T Philips

246   Intera Achieva, using a 32 channels coil. The experiments can be decomposed successively in three

247   "sessions" (about 1 hour each), "runs" (a few minutes), "blocks" (1 minute) and "events" (1 second).

248   One session was dedicated to retinotopic mapping and functional localizer runs using pictures of

249   objects, words and coloured stimuli (Mondrian). These latter runs were included to test whether

250   voxels involved in the decoding of synaesthetic colours were located in regions well-defined

251   functionally, respectively the Lateral Occipital Complex (LOC: Grill-Spector, Kourtzi, & Kanwisher,

252   2001), the Visual Word Form Area (VWFA: Dehaene & Cohen, 2011) and "colour centres" (Hupé et

253   al., 2012b). We did not have the opportunity to use those localizers (see Results). Retinotopic

254   mapping was performed strictly as described in a previous study (Bordier, Hupé, & Dojat, 2015),

255   using the Brain Voyager analysis pipeline to define in each subject the ventral and dorsal as well as

256   the left and right parts of areas V1, V2, V3 and V4 (ventral only). The parameters of the EPI functional

257   images were TR/TE: 2000/30 ms, excitation pulse angle: 80°, acquisition matrix: 80x80, bandwidth:

258   54.3 Hz/pixel, isotropic nominal resolution: 3 mm, 30*2.75 mm thick slices with 0.25 mm interspace

259   covering the whole visual cortex, with four additional dummy scans. To allow the precise alignment

260   of functional scans across sessions, a high-resolution structural image of the brain was also acquired

261   using a T1-weighted MP-RAGE sequence. The sequence parameters were TR/TE: 25/2.3 ms,

262   excitation pulse angle: 9°, 180 sagittal slices of 256*240 (read x phase), bandwidth: 542.5 Hz/pixel

263   isotropic nominal resolution: 1 mm, for a total measurement time of 4 min 31 s.

264   Another session was dedicated to the "synaesthesia" protocol (a structural image was also acquired

265   with the same parameters as in the first session, in the middle of the functional runs). Twelve

266   functional runs were acquired. The parameters of the EPI functional images were identical to those

267   used for the retinotopic mapping experiment but TR: 2500 ms for an acquisition volume of 45 slices

268   covering the entire brain with a total measurement time of 3 min 47 s. In each functional run, stimuli

269   of one type only were presented: letters, digits, concentric rings with the synaesthetic colours of

270   letters, or concentric rings with the synaesthetic colours of digits. The session contained three

271   successive sequences of four runs, each run with a different stimulus type (with a different random

272   order of stimulus type in each sequence). Each run contained 3*60 s blocks of a rapid-event

273   paradigm, separated by 10 s fixations. Stimuli of different "colours" were presented pseudo-

274   randomly in each block to optimize the estimation of the main effects. For example, in a letter block

275   for syn01 and her matched control, the letters E, N, V and A were presented six times each for 1 s,

276   with 1 s +/- 333 ms fixation only between each letter. This protocol allowed an estimation of the

277   BOLD response to each letter in each block (beta weights, using a General Linear Model, see below)

278   based on six presentations. We obtained three estimations (betas) in each run for each "colour", for

279   a total of thirty-six estimates (9 * 4 "colours") for each type of stimulus to be used by classifiers. The

280   power of classification algorithms depends on both the number and quality (signal to noise ratio) of

281   estimates (called exemplars). The present compromise between quantity and quality was based on

282   (Mumford, Turner, Ashby, & Poldrack, 2012) and on preliminary experiments (Ruiz, Hupé, & Dojat,

283   2012). Subjects had to fixate the centre of the screen (the fixation point, present between stimuli and

284   at the centre of the coloured rings, or the centre of the grapheme) and pay attention to the stimuli

285   for the whole duration of each run. To help subjects maintain attention, they performed a one-back

286   task (pressing a button each time the same stimulus was repeated twice in a row).

287   In the remaining session, a high-resolution, high-contrast structural image of the brain was acquired

288   using a T1-weighted MP-RAGE sequence. The sequence parameters were TR/TE/TI: 25/3.7/800 ms,

289   excitation pulse angle: 15°, acquisition matrix: 180 sagittal slices of 256*240 (read x phase),

290   bandwidth: 191 Hz/pixel, readout in anterio-posterior direction, number of averages: 1, sense factor

291   anterio-posterior: 2.2, right-left: 2, isotropic nominal resolution: 1 mm, with a total measurement

292   time of 9 min 41 s. This image was the structural reference image of each subject. We also acquired

293   diffusion-weighted images, analysed in another study (Dojat, Pizzagalli, & Hupé, 2018) and a

294   sequence of functional resting state (not analysed yet).

295   We recorded oculomotor signals during the scans with an ASL EyeTracker 6000. At the beginning of

296   each session, subjects had to fixate each point of a calibration matrix, and were therefore aware that

297   the quality of their fixation was monitored. However, signal quality in some subjects was not good

298   enough or not constant, or even too poor to be of any use for subjects who had to wear non-

299   magnetic glasses in the scanner, so we did not even attempt to analyse these data. We can only

300   speculate that subjects had a better fixation than if they did not know that their gaze was recorded.

301   Whole brain univariate analyses did not reveal any activation along the anterior calcarine and the

302   parieto-occipital sulcus, where activations correspond to the signature of blinks (Hupé, Bordier, &

303   Dojat, 2012a), providing indirect evidence that the distributions of blinks were not correlated with

304   our stimuli presented randomly.

305   **Data Analysis**

306   The standard pre-processing procedure of functional images was applied using SPM8: slice-timing

307   correction, then motion correction with realignment, together with correction of spatial distortions

308   of the static magnetic field (Vasseur et al., 2010). The within session structural image was realigned

309   to the mean EPI image, as well as the high resolution high contrast structural image, but no further

310   transformation of the EPI images was performed. No spatial smoothing was applied for MVPA, as

11

311   maximally differential activation of voxels was shown to maximize the power of classifiers (Ruiz et al.,

312   2012). This was confirmed on these data when testing spatial filters with FWHM = 3, 6 and 9 mm.

313   Transformation matrices were computed between the structural image and the MNI template to

314   allow the transformation and projection of atlas-based masks of specific anatomical structures

315   (Anatomy Toolbox for SPM8 Version 2.2b, 2016) into the subject's space.

316   For MVPA (our main analysis), for each subject and each run we first ran a General Linear Model

317   (GLM). The six parameters of motion correction were included as factors of non-interest in the design

318   matrix. Thirteen main predictors, four events (grapheme or colour) * three blocks plus one for when

319   only the fixation point was shown, were obtained by convolving the canonical HRF with Dirac

320   functions corresponding to the time of presentation of each stimulus. The corresponding beta

321   weights estimated by the GLM for each colour (real or synaesthetic) and stimulus type (ring or

322   grapheme), divided by the square root of residuals, were used as examples by a Support Vector

323   Classification (SVC) algorithm (Scikit-learn version 0.15.2, implemented in Python version 2.7.9.0:

324   Pedregosa et al., 2011). We used a linear kernel (default value of the C parameter = 1) and a one-

325   versus-one classification heuristic to classify each example in one of the four categories. For all five

326   classifications describes below, training and test runs were always fully independent: betas obtained

327   from blocks from the same run were never split between training and test runs.

328   **Classifications.** We trained and tested five families of classifiers (Figure 3). Six runs (eighteen blocks)

329   were used for colour ('Col' family of classifiers) and synaesthesia ('Syn') decoding. The procedure was

330   leave-one-run-out. Six classifiers were therefore trained to classify (5 runs * 3 blocks * 4 colours = 60)

331   colour exemplars in four categories, and tested on (1 run * 3 blocks * 4 colours = 12) independent

332   exemplars. Performance was therefore computed over seventy-two classifications (6 classifiers * 12

333   tested exemplars), with chance level = 25% and 95% Confidence Interval of chance for each subject =

334   [16 36]% (binomial probability, Agresti-Coull estimation). For grapheme runs, training was performed

335   on pairs made of one letter and one digit. If the decoder learnt only the letters, for example (by being

336   able to filter out the responses to digits), then performance on decoding letters and digits could

337   reach up to 50%, without knowing anything about synaesthetic colours. One could expect, however,

338   that performance of synaesthetes would be higher than for controls because of the additional

339   information provided by synaesthetic colours. A more stringent test of synaesthetic coding ('g1g2')

340   was the training of one classifier on letters (3 runs * 12 exemplars) and testing on digits (and the

341   reverse). Learning was achieved using thirty-six exemplars (letters or digits) to be classified in four

342   categories, test was on thirty-six exemplars (digits or letters), for a total performance over seventy-

343   two classifications by combining training on letters and training on digits. To evaluate if brain regions

344   coded both real and synaesthetic colours ('C2S'), training was performed by one classifier on six

12

345   colour runs (seventy-two exemplars), test on six grapheme runs (seventy-two exemplars). We also

346   performed the reverse classification ('S2C').

347
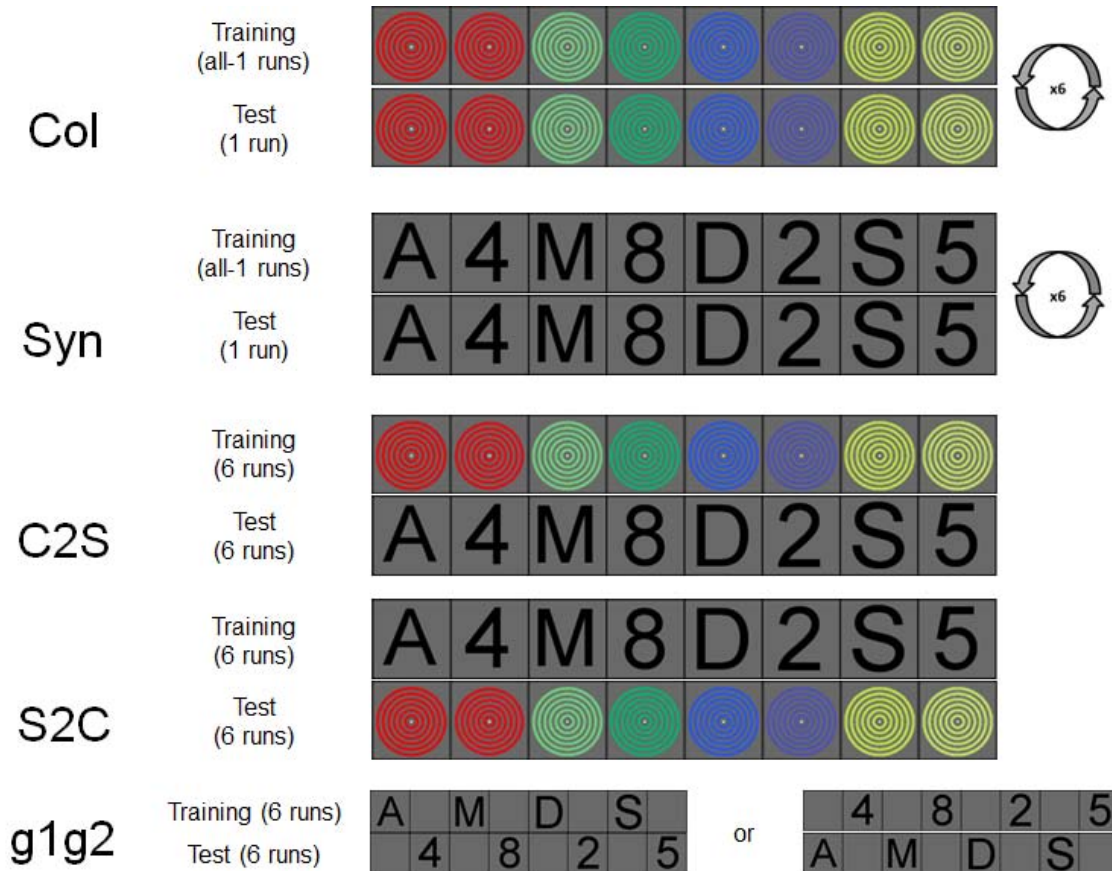
348

349   **Figure 3.** MVPA classifications. 'Col' classification: The procedure was leave-one-run-out. Six classifiers were trained to

350   classify 60 colour exemplars from 5 runs in four categories, and tested on 12 independent exemplars of the remaining run.

351   Performance was therefore averaged over seventy-two classifications (6 classifiers * 12 tested exemplars). 'Syn'

352   classification: The procedure was the same as for the 'Col' classification, based on pairs of graphemes and therefore also

353   synaesthetic colours for synaesthetes. 'C2S' classification: Training was performed by one classifier on six colour runs

354   (seventy-two exemplars), test on six grapheme runs (seventy-two classifications). 'S2C' classification: The procedure was

355   the same as for the 'C2S' classification. 'g1g2' classification: Classifiers were trained on letters (3 runs * 12 exemplars) or

356   digits (3 runs) and tested respectively on digits or letters. Overall performance was based on seventy-two classifications.

357

358   We computed MVPA in regions of interest (ROIs) defined in each native (non-transformed) subject

359   space. We used visual areas defined by individual retinotopic mapping as well as atlas-based ROIs

360   (Figure 4). We expected synaesthetic colours to involve the ventral visual pathway, anterior to V4, so

361   we tested the four subdivisions of the fusiform gyrus (FG, Figure 4a). Some studies have also

362   suggested the role of parietal areas, even though no consensus emerged about exactly which part if

363   any may be involved (Hupé & Dojat, 2015), so we defined ROIs in parietal regions (Figure 4b).

364
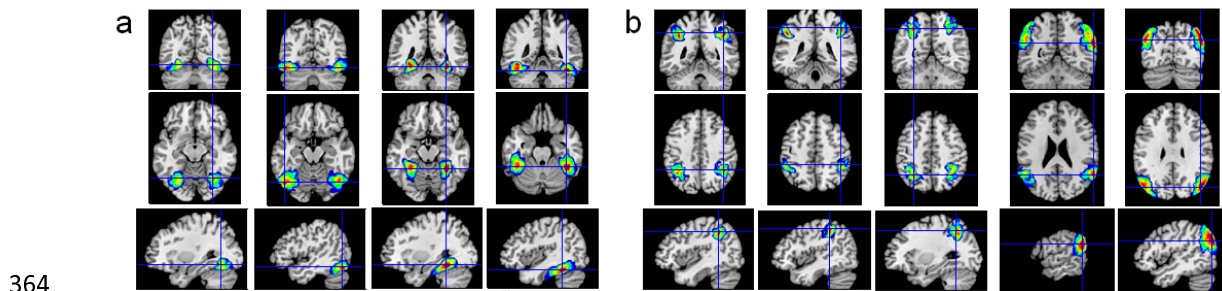
Figure 4. a. Atlas-based regions of interest (ROI) of the fusiform region. From left to right, FG1, FG2, FG3 and FG4. Colour gradients denote the probability of being in the specified ROI, from 0% (dark blue) to 100% (dark red). We considered the largest ROI as the mask of the corresponding region. **b.** Parietal ROIs. From left to right, AIPS_IP1, AIPS_IP2, AIPS_IP3, IPL_PGa and IPL_PGp. See text for full names and references of these areas.

369

370   For each subject, anatomical ROIs were defined as the intersection of the subject's grey matter mask

371   and the mask of the anatomical ROIs (Anatomy Toolbox for SPM8: Eickhoff et al., 2007) projected

372   into the subject's space. Both retinotopic and atlas-based ROIs had different number of voxels within

373   and across subjects. The performance of classifiers may depend on the number of voxels (called

374   "features" for the algorithm), making difficult the comparison of absolute performance in different

375   ROIs. Between-subject differences may also bias group comparisons.

376   To address this issue, we first tested ROIs of different sizes by regrouping retinotopic areas and

377   subdivisions of the fusiform areas and of the parietal areas. The pattern of results were similar

378   whatever our grouping choice of ROIs. We present the results for ROIs of intermediate size (we

379   indicate the min and max number of voxels across subjects in each ROI), regrouping the right and left

380   parts of retinotopic areas (V1 = [206 441], V2 = [125 420], V3 = [156 340], V4 = [94 268]), the two

381   posterior (J. Caspers et al., 2013) (left = [98 150], right = [61 125]) and anterior (Lorenz et al., 2017)

382   (left = [174 331], right = [127 271]) parts of the fusiform areas, the 3 subdivisions of the Intaparietal

383   Sulcus (Choi et al., 2006; Scheperjans et al., 2008) (left = [197 311], right = [191 275]) and the anterior

384   and posterior parts of the Inferior Parietal Lobule (S. Caspers et al., 2006; S. Caspers et al., 2008) (left

385   = [131 335], right = [124 279]).

386   We also defined ROIs using the same number of voxels in each subject and ROI. To do that, for all

387   classifications, we selected 100 voxels with the highest F-scores to colours in each area (we tested

388   different selection sizes and found that 100 was about the optimal number of voxels to reach

389   maximum performance). In order to have enough voxels to choose from in every subject, we

14

390   selected voxels in only six large areas: the left and right retinotopic areas V1 to V4 (minimum number
391   of voxels across subjects were respectively 352 and 327), the left and right fusiform areas FG1 to FG4
392   (298 and 188) and the left and right parietal areas (347 and 315). Such a selection provides the best
393   chances for colour classifiers (since we select voxels maximally modulated by colours), but
394   classification is then not independent of selection when measuring colour decoding after selection of
395   F-scores to colours (but classification is independent for grapheme decoding). In order to provide a
396   fair measure of colour decoding performance to compare grapheme decoding with, voxels were
397   selected using F-values computed based only on runs used for training, meaning that each of the six
398   training sets was based on a different set of voxels. For other classifications, the same set of voxels
399   was used based on F-values computed across all colour runs.

400   **Statistical analysis**

401   In each ROI, we computed 95% CIs of the performance of each group, as well at the 95% CIs of the
402   between group differences. We performed both independent and paired comparisons. Paired
403   comparisons are in principle more appropriate and powerful with this protocol, because it cancels
404   any difference due to the specific choice of colours and graphemes; however, for voxels not
405   concerned with those small differences, pairing is artificial and may just bring some noise. Results
406   were in any case very similar for both comparisons. We show the CIs for paired comparisons. We also
407   performed paired comparisons by computing the 95% CI of the odds ratio when comparing 19
408   synaesthetes against their matched controls, using a mixed-effect generalized linear model, with a
409   binomial family and a logit link function, as implemented in the library lme4 (Bates, Mächler, Bolker,
410   & Walker, 2015) in R, version 3.3.3.

411   In order to fully exploit our data set, we performed two additional analyses.

412   A searchlight analysis was performed over the whole brain (Kriegeskorte et al., 2006). Whole brain
413   analyses are in principle less powerful than ROI analyses because they constrain to distort each
414   subject's anatomical space within one common space, so the average performance at any given voxel
415   may in reality correspond to different anatomico-functional voxels in different subjects. Moreover,
416   they re-introduce the methodological issues related to spatial smoothness (Stelzer, Lohmann,
417   Mueller, Buschmann, & Turner, 2014). This analysis was therefore exploratory. It allowed us to
418   discover other clusters potentially involved in synaesthesia, which we could further analyse as post-
419   hoc regions of interest to see if they displayed a consistent pattern of results across classifiers. The
420   searchlight analysis used a 15 mm radius and the SVC algorithm. Performance maps were
421   transformed to the common DARTEL space for voxel-wise group comparisons (resolution 3 by 3 by 3
422   mm). We performed in SPM8 two-sample (groups of 20 subjects) and paired-sample t-tests (N = 19)

15

423   between synaesthetes and controls, as well as one-sample t-tests to compare the average

424   performance of each group (N = 20) against chance (= 0.25). For all comparisons, no individual voxel

425   reached pFWE < 0.05. We used cluster-based statistics with the cluster-forming threshold set to p =

426   0.001 and pFWE < 0.05.

427   We also performed whole-brain univariate analyses on the groups of synaesthetes and controls to

428   test for differences of magnitude of the BOLD responses to graphemes evoking synaesthetic colours.

429   The design of the experiment was not optimized for these analyses since we did not have any control

430   stimuli (those being not necessary for MVPA). The rationale was the same as for the whole brain

431   searchlight analysis: if any difference was found between synaesthetes and controls, the revealed

432   clusters could be defined as post-hoc regions of interest for our classifiers to test if those regions

433   were involved in coding synaesthetic colours. A 9 mm FWHM spatial smoothing was applied to the

434   subjects' EPI images before testing two contrasts: a T-contrast of all stimuli against the fixation point

435   (we did not have graphemes that did not evoke any synaesthetic colour); an F-contrast of the four

436   pairs of graphemes. Contrast maps were distorted within the study-specific template computed using

437   DARTEL procedure as implemented in VBM8 (Dojat et al., 2018) and to the MNI space (resolution 1.5

438   by 1.5 by 1.5 mm). For second-level analyses, we compared the contrast maps of synaesthetes (N =

439   20) against controls (N = 20) using t-tests (testing stronger signals either in synaesthetes or controls).

440   We also performed paired t-tests on 19 synaesthetes against their matched control to account for

441   possible differences due to the specific choices of graphemes in each synaesthete. For all

442   comparisons, no individual voxel reached p < 0.05, corrected for the family-wise error (FWE, based

443   on the random field theory as implemented in SPM8). We used cluster-based statistics with the

444   cluster-forming threshold set to p = 0.001 (Eklund, Nichols, & Knutsson, 2016) and pFWE < 0.05. As a

445   final control analysis, we performed the same analyses for coloured stimuli.

446   **Data Availability.** The datasets generated and analysed during the current study are freely available

447   on request (https://shanoir.irisa.fr/Shanoir/login.seam), contact M. Dojat. The data are not publicly
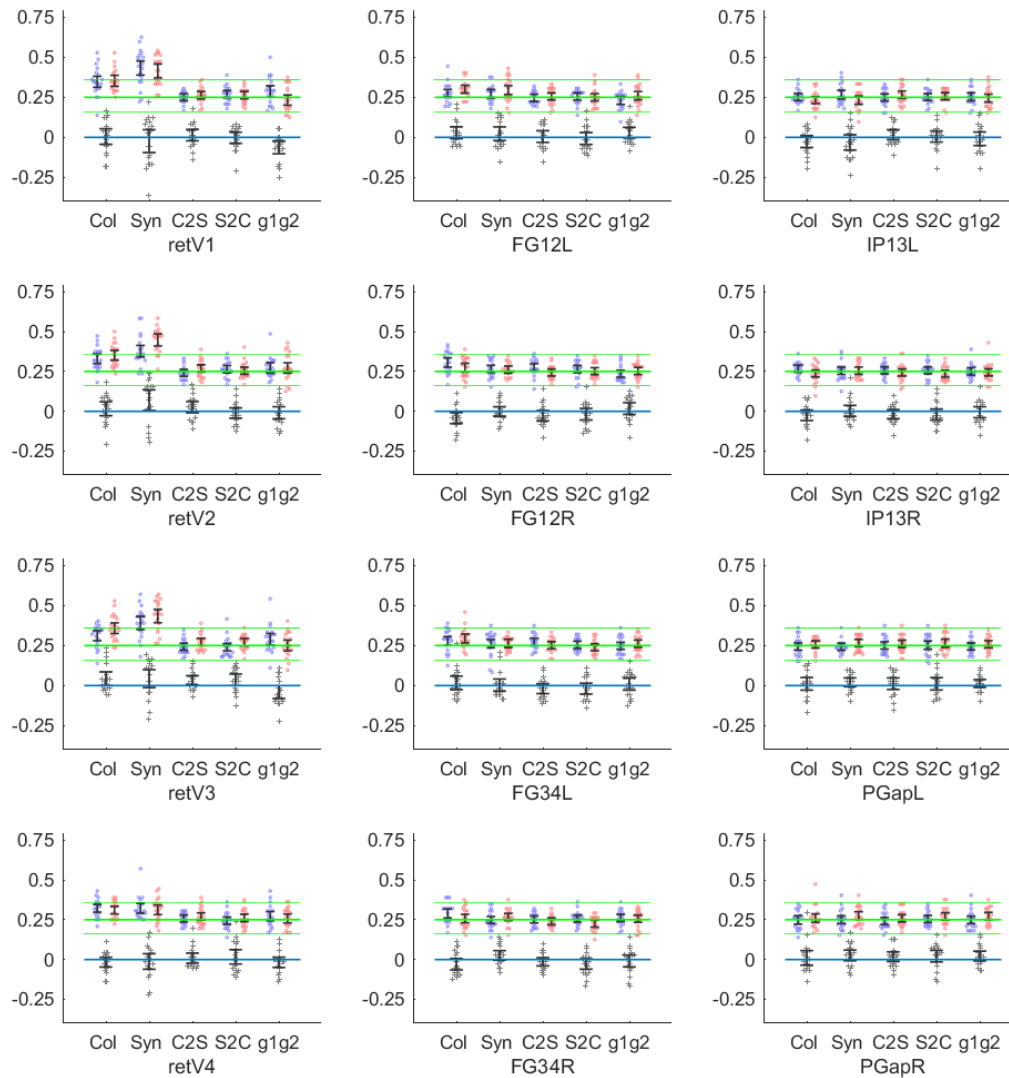
448   available due to privacy restrictions.

449

450

451   **Results**

452   **Multivariate pattern analysis in regions of interest (defined at the individual level)**

453   Figure 5 shows the performance of all classifiers (described in Figure 3) in all our ROIs, without any

454   voxel selection (ROIs have therefore different number of voxels across regions and subjects).

Figure 5. Performance of classifiers in retinotopic areas, the fusiform gyrus and parietal areas. Each ROI regrouped several areas, for example the left and right parts of V1 for 'retV1' in order to provide a large number of voxels in each subject and ROI (at least > 60, and > 100 voxels in most ROIs; see Methods: Data Analysis). 'retV1' to 'retV4' were defined based on retinotopic mapping in each subject; other ROIs were defined as the intersection of the subject's grey matter mask and the mask of atlas-based anatomical ROIs (Anatomy Toolbox for SPM8) projected into the subject's space (see Figure 4). FG12L = left (FG1 + FG2), IP13L = left (AIPS_IP1 + AIPS_IP2+ AIPS_IP3), PGapL = left (IPL_PGa + IPL_PGp), etc. Each classifier was trained and tested on beta weights computed on voxels in the native subject space with no spatial smoothing. Each panel displays the individual and average performances of five classifiers (see Figure 3): 'Col' = training and test on betas for real colours (rings); 'Syn' = training and test for synaesthetic colours (graphemes, letters or digits); 'C2S' = training on real colours (rings) test on synaesthetic colours (graphemes); 'S2C' = training on synaesthetic colours test on real colours; 'g1g2' training on letters test on digits or training on digits test on letters. The y-axis represents both the *performance* of classifiers (between 0 and 1, chance level = 0.25, thick green line; 95%CI of chance for each subject = [0.16 0.36], thin green lines) for individual subjects (blue = controls, red = synaesthetes) and their group average (with 95% Confidence Intervals) and the *difference of performance* (grey crosses) between synaesthetes and their matched controls (0 = no difference between groups, blue line; whiskers denote 95% CI).

471   In each subplot, the first two beeswarms from the left show the performance of decoders in each

472   subject for real colours ('Col' classification). As expected, the decoding of real colours was above

473   chance (0.25, thick green line) in retinotopic areas as well as in the fusiform gyrus for both controls

474   (blue points) and synaesthetes (red points). No difference was expected nor observed between

475   groups (whiskers across the zero blue line denote the 95% CI for paired comparisons of performance

476   of 19 synaesthetes against their matched control, the difference of performance being denoted by

477   the grey crosses). Note though that the whole 95% CI was slightly above 0 in retinotopic V3, 'retV3',

478   and it was slightly below 0 in the subdivisions 1 and 2 of the right fusiform gyrus, 'FG12R' (differences

479   are more visible when estimating the CI by a mixed-effect generalized linear models: Supporting

480   Information, Figure S4). But without any independent evidence, these small differences could be due

481   to random sampling. Indeed, all the 99.58% CIs included 0 (Bonferroni correction over 12 tests).

482   The next beeswarms are for the classification of pairs of graphemes. In synaesthetes only,

483   classification could in principle be achieved based on the synesthetic colours, since the synesthetic

484   colour was the main shared feature associated to each grapheme pair (in most cases one letter and

485   one digit) had in common (so we called it the 'Syn' classification). For example, E and 7 were both

486   associated to red by syn01 (see Figure 1). Performance was above chance level (25%) in controls. This

487   means that this performance could be achieved by classifiers based on either some spatial features

488   shared by each grapheme pair or by optimizing decoding to only one of the graphemes. In order to

489   test whether graphemes could be decoded on the basis of synaesthetic colours, we looked if

490   synaesthetes performed better than controls. This was the case in retinotopic V2 (95% CI of the

491   difference of performance, two-sample t-test: [1.5 12.5]%; paired t-test: [0.5 13.4]%; 95% CI of the

492   odds ratio = [1.15 1.56]; see Methods, statistical analysis) and to a lesser extent in retinotopic V3 (but

493   note that performance was lower for synaesthetes in the subdivisions 1 to 3 of the left Intra-Parietal

494   Sulcus, IP13L; such a difference is most likely due to random sampling since none of the group

495   performances in IP13L was above chance). Only the difference in V2 survived Bonferroni correction

496   over 12 tests, for the mixed-effect analysis (p = 0.0002).

497   The third group of beeswarms represent the data answering our main question: can synaesthetic

498   colours be decoded based on real colours ('C2S' classification)? This was not the case in any ROIs we

499   considered in controls, as expected, but also in synaesthetes (the 95% CI of all groups crossed the

500   0.25 chance baseline). In particular, performance was not significantly above chance in V2, as would

501   have yet been expected if the higher performance in synaesthetes for the 'Syn' classification was

502   really due to the coding of synaesthetic colours. Moreover, there was no evidence of better

503   classification in synaesthetes than controls. We obtained similar null results when we tried to decode

504   real colours based on graphemes (and possibly synaesthetic colours in synaesthetes: 'S2C'

505   classification).

506   The last beeswarms on the right of each subplot show the performance for another classification that

507   should have been possible only on the basis of synaesthetic colours: classifiers were trained on one

508   set of graphemes (digits or letters) and tested on the other set of graphemes ('g1g2' classification).

509   Again, performance was never above chance and we found no difference between groups, in

510   particular in V2. We even observed lower scores for synaesthetes in V1 (where it even survived

511   Bonferroni correction for the mixed-effect analysis: $p = 0.0002$) and V3, where we had yet observed

512   higher performance for 'Syn' decoding. This lack of consistency across different tests addressing the

513   same question confirmed that these small variations, even when statistically "significant", were most

514   likely due to random sampling.

515   We performed again all these analyses using six larger ROIs (regrouping either the left or the right

516   parts of V1 to V4, FG1 to FG2 and the areas of the inferior parietal lobule and the intraparietal sulcus)

517   in which we selected the 100 voxels with the largest scores to F-tests to real colours, in order to feed

518   the classifiers with the voxels most sensitive to real colours (Figure 6). The performance of the 'C2S',

519   'S2C' and 'g1g2' classifiers was never above chance in synaesthetes (nor in controls, as expected),

520   and performance was never better in synaesthetes.
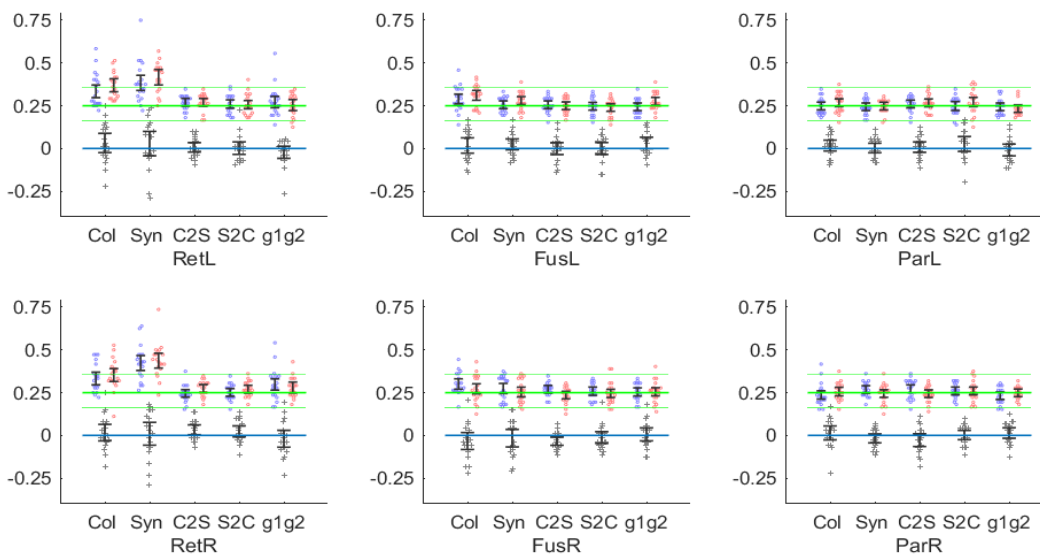
521

522   **Figure 6.** Performance based on the same number of voxels (= 100) in each large ROI (retinotopic areas, fusiform gyrus and

523   parietal regions) and subject. For the classification of real colours ('Col'), the selection of the best F-values to colours was

524   different for each of the six leave-one-out classifications, based each time only on the five runs used for training the

525   classifier, to insure independence of training and test. For the other selections, all colour runs were used to select the

526   voxels with the highest F-scores. The high performance for the 'Syn' classification in retinotopic areas indicates that many

527   voxels respond both to change of colour or luminance and the shape of graphemes, probably thanks to the small receptive

19

528   fields of lower visual areas. Same conventions as in Figure 5. The CIs of the odds ratio computed by mixed-effect

529   generalized linear models are shown in Supporting Information, Figure S5.

530   **Individual differences**

531   The phenomenological experience of synaesthetic colours may vary a lot across synaesthetes, which

532   may compromise the visibility of effects at the group level. While this phenomenology has been so

533   far problematic to capture with objective measures, we could estimate the strength of the

534   synaesthetic associations in each subject, using variants of Stroop tasks. We reasoned that

535   synaesthetes with stronger synaesthetic associations might have stronger modulations of the BOLD

536   signal and thus larger decoding values. We first tested area V2, where we had observed on average

537   higher performance in synaesthetes for the 'Syn' classification. We were wondering if this higher

538   performance was really due to the coding of synaesthetic colours, because our other, more specific

539   classifiers ('C2S', 'S2'C and 'g1g2'), had not revealed any difference. A correlation between

540   synaesthetic strength and performance would constitute an independent validation of coding. Figure

541   7 shows the performance of each subject as a function of the strength of synaesthetic associations,

542   measured in Stroop-like psychophysics experiments (see Table 1 and Ruiz & Hupé, 2015, for further

543   explanations about the 'Photism Strength' index) for synaesthetes only (red crosses). Controls (blue

544   circles) were attributed the value of their matched synaesthete.
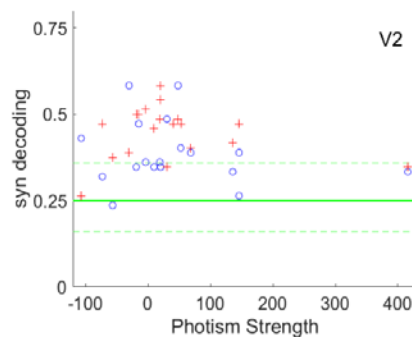
545

546   **Figure 7.** Performance of the classifier trained and tested with synaesthetic colours (pairs of graphemes) in each subject in

547   area V2 defined retinotopically (same data as 'Syn' in the second panel of the first column of Figure 5) as a function of the

548   strength of synaesthetic associations ('Photism Strength'). This strength, measured for synaesthetes (red crosses), does not

549   show any evidence of correlation with the performance of the 'Syn' decoder ($r = -0.11$, 95% CI = [-0.54 0.36]). Controls (blue

550   circles) were attributed the value of their matched synaesthete ($r = -0.18$, 95% CI = [-0.58 0.30]). Note that one value of

551   Photism Strength was larger than the other ones. We carefully checked that this value was correct. However, given its

552   possible influence on the correlation results, we complemented this analysis with two other analyses, by removing this

553   value (for synaesthetes, $r = 0.28$, 95% CI = [-0.21 0.66]) and by performing non-parametric correlations (Spearman $r = -0.03$,

554    $N = 19$, $p = 0.90$). We compared the results of these three statistical tests for all the other tested correlations. The statistical

555   conclusions were always similar, except for one case described in Supporting Information, Figure S2.

556   There was no correlation between both measures, neither for synaesthetes nor, as expected, for

557   controls. We also observed that the difference of score between each synaesthete and her (or his)

558   matched control did not increase with photism strength (r = 0.06, 95% CI = [-0.42 0.52]; Spearman r =

559   0.01, N = 18, p = 0.95). Therefore, this analysis did not provide any independent argument in favour

560   of the decoding of synaesthetic colours in V2. We computed similar correlation analyses in every ROI

561   and for all classifiers and never found any correlation (all uncorrected p > 0.05). We also computed

562   both positive and negative correlations over the whole brain for the five classifiers, independently for

563   synaesthetes and controls. We never found any significant cluster (cluster forming threshold, p =

564   0.001).

### Whole brain searchlight multivariate pattern analysis

566   We complemented our ROI analysis with searchlight analyses over the whole brain (normalized to

567   the MNI space), comparing the performance of each group against chance as well as comparing

568   groups for the five classifications. These exploratory analyses were performed to discover clusters

569   potentially involved in synaesthesia outside of our ROIs. "Significant" clusters could be used as post-

570   hoc regions of interest to see if they displayed a consistent pattern of results across classifiers (these

571   results are displayed in Supporting Information, Table S1). We found no differences between controls

572   and synaesthetes at our statistical threshold for classifiers trained and tested on colours (rings, 'Col'

573   classifiers). For classifiers trained and tested on synaesthetic colours (graphemes, 'Syn' classifiers),

574   we observed higher performance in synaesthetes in the parietal cortex (Table S1: on the right side

575   with paired t-tests and on the left side with two-sample t-tests; bilateral difference could be

576   observed for both contrasts when using a higher cluster-forming threshold). However, testing

577   synaesthetes against chance revealed no cluster at our threshold around these coordinates of the

578   parietal cortex (performance was above chance in both groups in the occipital cortex, as expected).

579   We found no difference between controls and synaesthetes at our statistical threshold for the critical

580   test of shared coding of real and synaesthetic colours, when classifiers were trained on coloured

581   rings and tested on graphemes ('C2S' classifiers). Testing synaesthetes against chance also revealed

582   no cluster. The reverse classification (learning on graphemes, 'S2C'), however, revealed two clusters

583   with higher performance in synaesthetes for independent t-tests, in the right occipito-temporal

584   cortex and in the left putamen. Only the first cluster was confirmed by paired-comparisons. When

585   testing performance against chance two clusters emerged for synaesthetes (none for controls), one

586   again in the same part of the right occipito-temporal cortex, and the other in the left parietal cortex,

587   abutting the parietal cluster obtained previously for the higher performance in synaesthetes for the

588   'Syn' classification (we shall come back to this concordance in the following *post-hoc* analysis).

589   Finally, for classifiers trained on either letters or digits (and tested respectively on either digits or

590   letters), a critical test of the coding of synaesthetic colours, higher performance was observed, but in

591   controls, in the left inferior frontal gyrus, for both paired and independent t-tests. However, no

592   cluster emerged anywhere in the brain in controls (nor in synaesthetes) when testing performance

593   against chance, so this cluster should be considered as a false positive.

594   *Post-hoc* analysis. We further explored the performance of classifiers in the two clusters identified by

595   the 'Syn' classifier and the five clusters identified by the 'S2C' classifier, corresponding in fact to two

596   parietal regions (left and right), one right occipito-temporal region and one cluster in the left

597   putamen. In each cluster, we computed the average across voxels of the searchlight scores, in order

598   to compare the performances of our five classifiers for synaesthetes and controls in these seven

599   clusters defined *post-hoc*, with two-sample and paired-sample t-tests. We also compared the

600   performance of each group against chance. Statistically "significant" differences were obtained only

601   for the contrasts used to define the clusters (Table S1). Only one additional comparison was

602   "significant" (p = 0.012, not corrected for multiple comparisons) in the left parietal cluster at XYZ = [-

603   33 -28 50], which had been obtained when testing synaesthetes against chance for the 'S2C'

604   classification (training classifiers on graphemes and testing them on colours: Figure 8): synaesthetes

605   also performed better than controls at decoding graphemes ('Syn' classification), 95%CI = [1 9]%

606   (paired comparisons), and better than chance (95% CI = [26 31]%), but the performance was not

607   correlated with the strength of synaesthetic associations (p = 0.51).

608
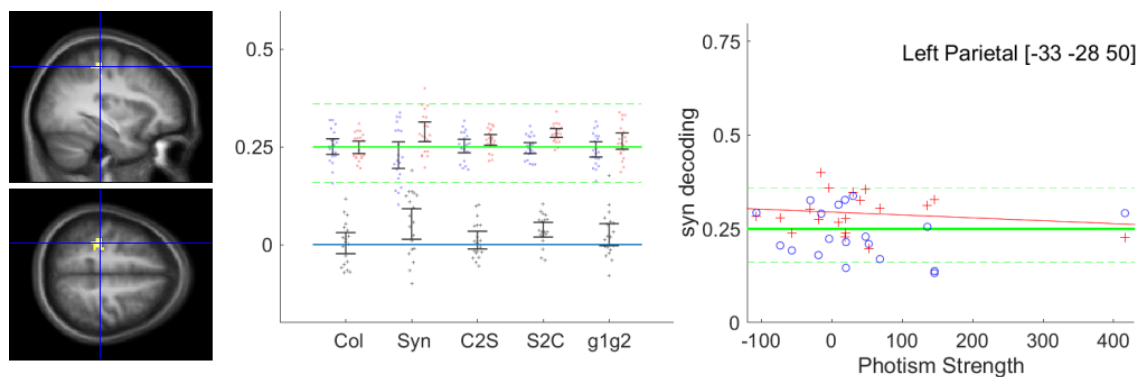
609
610   **Figure 8. Left**: Parietal cluster identified based on whole brain searchlight analysis for 'S2C' decoding, Synaesthetes>chance

611   (27-voxel cluster at XYZ = [-33 -28 50], one-sample t-test). **Middle**: performance of classifiers in this cluster (same

612   conventions as in Figure 5). The performance of synaesthetes was logically above chance for the 'S2C' classification, since

613   the cluster was defined based on this contrast. For the independent classifier 'Syn', the performance of synaesthetes was

614   also above chance and above that of controls. **Right**: Absence of correlation between the strength of synaesthetic

615   associations and 'Syn' decoding (Spearman r = 0.02, N = 19, p = 0.95; for 'S2C' decoding, not shown: Spearman r = -0.15, N =

616   19, p = 0.53).

617 **Whole brain univariate analyses (normalized anatomical space)**

618 Similarly to the searchlight analyses, these whole-brain univariate exploratory analyses were
619 performed to discover clusters potentially involved in synaesthesia outside of our ROIs. They
620 revealed no difference between controls and synaesthetes at our statistical threshold for T-contrasts
621 of graphemes when performing two-sample t-tests. However, the paired-sample t-tests revealed
622 stronger BOLD signal in a small cluster in synaesthetes, close to the left precentral gyrus. We treated
623 this cluster as a candidate region for the coding of synaesthetic colours (Supporting Information,
624 Table S1).

625 For F-contrasts, we did not observe any stronger modulation in synaesthetes (neither for two-sample
626 nor paired-sample t-tests). Surprisingly, we observed stronger modulation in controls in two clusters
627 (paired comparisons), in the right occipito-parietal cortex (Supporting Information, Figure S1) and in
628 the left insula. The two-sample t-tests revealed only the occipito-parietal cluster. We did not have
629 any explanation for these differences, which might be false-positives (Eklund et al., 2016). We note
630 that the analysis by (Rouw & Scholte, 2010) revealed a cluster (which they called IPS, cluster extent =
631 3280 mm3) at equivalent peak coordinates on the left side ([-30 -72 28]), obtained with the contrast
632 synaesthetes>controls for (synaesthetic graphemes)>(non-synaesthetic graphemes). In our case, the
633 weaker modulation by graphemes in synaesthetes would rather argue against the hypothesis of a
634 functional role of this region in synaesthesia. We included these two regions in our post-hoc MVPA
635 analyses for further exploration.

636 We also tested T- and F-contrasts for the responses to real colours (rings). We observed stronger
637 BOLD signal (T-contrast) in synaesthetes only, in three clusters for paired comparisons (in the left
638 posterior and anterior insula – see Supporting Information, Figure S2 - and in the left
639 parahippocampal region) and two other clusters for two-sample t-tests (in the right middle temporal
640 gyrus and in the right superior, medial, frontal gyrus - see Supporting Information, Figure S3). The
641 lack of consistency between paired and two-sample t-tests could again suggest false-positives, but
642 we nonetheless included these five clusters in our post-hoc MVPA analyses, in case those stronger
643 activations be related to the implicit activation of graphemes by the colours associated to them ("bi-
644 directional" synaesthesia: Gebuis, Nijboer, & Van der Smagt, 2009). F-contrasts to colours revealed
645 only one cluster of stronger modulation in controls in the frontal region, but in the middle of white
646 matter and thus clearly a false positive.

647 We compared the performances of synaesthetes and controls for our classifiers in those eight
648 clusters defined post-hoc, with two-sample and paired-sample t-tests. Only three comparisons came

649   out "significant" at $p < 0.05$, but without correction for multiple comparisons (Table S1). Supporting

650   Information, Figs. S1 to S3 detail the results obtained in these three post-hoc clusters.

651

Discussion

653   Our goal with this study was to provide univocal evidence of the activation of the 'colour network' by

654   imaginary colours as experienced by grapheme colour synesthetes.

655   Studies based on univariate analyses to search the neural correlates of synaesthetic colours face two

656   major problems. First, BOLD responses to stimuli leading to the experience of synaesthetic colours

657   need to be compared to a control response (subtraction method: see the Figure 1 by Hupé & Dojat,

658   2015). Such a control response may be obtained by testing the same subjects with similar stimuli that

659   do not generate a synaesthetic experience (pseudo-graphemes or graphemes that, by chance, do not

660   generate such an experience in the tested synaesthetes). The problem is, it is impossible to know

661   whether the additional activations, if observed, are specific to the synaesthetic experience of colours.

662   For example, letters and numbers can also be named, unlike pseudo-graphemes. A control response

663   may also be obtained by testing non-synesthetes with the same stimuli. But, again, it is impossible to

664   know whether the additional activations, if observed, are specific to the synaesthetic experience of

665   colours. For example, synaesthetes often enjoy visualizing the synesthetic colours of graphemes:

666   attentional and emotional components may therefore bias the comparison. Second, averaging the

667   results across subjects require to transform the individual data within a common reference space,

668   with the possible loss of fine-grained spatial information. The first problem may generate false

669   positive results, the second false negative results.

670   Thus, because univariate analysis led to inconsistent results (Hupé & Dojat, 2015), we used in this

671   study Multivariate Pattern Analysis (MVPA) on 20 synaesthetes and 20 control participants, to

672   explore whether the neural processing of real colours and synaesthetic colours shared patterns of

673   activations. To our knowledge, it was the first time that MVPA was proposed in this context. By using

674   MVPA, we could in principle overcome problems associated with univariate analysis because we test

675   the performance, in each individual, related to the coding of certain attributes, not a level of

676   activation in need of further interpretation. Our design was optimized to test if classifiers, trained to

677   distinguish patterns of responses to four different real colours in groups of voxels from different

678   regions of the brain, could classify above chance the responses of those voxels to achromatic

679   graphemes leading to the synaesthetic experience of the exact same colours. The logic was that only

680   synaesthetes tested with their exact, idiosyncratic, synaesthetic code could produce above-chance

681   performance. Unfortunately, the performance of our group of 20 synaesthetes remained very close

24

682   to chance (all $p < 0.05$, uncorrected) in all our selections of voxels (retinotopic areas defined at the

683   individual level as well as the fusiform gyrus and parietal regions of interest defined based on a

684   probabilistic atlas), and whatever the extent of the chosen areas or the selection method of the

685   voxels (Figure 5 and 6, classification 'C2S' in synaesthetes shown by red points).

686   A statistical comparison revealed that the performance of synaesthetes was also no better on

687   average than that obtained in control subjects. Of course, the absence of statistically significant

688   effect cannot lead to conclude to the absence of effects. The null result could be due to a lack of

689   power, if, for example, only a few synaesthetes had reached a good performance. However, the

690   results were striking when inspecting the distributions of individual performances: the scores of most

691   synaesthetes were distributed around the chance level, and almost no synaesthete reached an

692   individual performance above the chance level (binomial probability: all the points are included

693   within the green dotted lines). The correlation analyses with a measure of individual differences (the

694   strength of the synaesthetic associations) further confirmed the homogenous performance of

695   synaesthetes around chance. Under our experimental conditions, the collected data therefore do

696   show quite convincingly the absence of shared coding of real and synaesthetic colours.

697   We further analysed our data set in different ways, in order to be able to detect some signs of coding

698   of synaesthetic colours by neural networks not involved in the coding of real colours. The 'g1g2'

699   classification, which could have been achieved only on the basis of shared synaesthetic colours

700   across letters and digits, remained at the chance level in synaesthetes. The 'syn' classification,

701   expected to reach a higher performance in synaesthetes, was similar in controls. We also explored

702   the performance of classifiers beyond our regions of interest, across the whole (normalized) brain

703   (searchlight analysis) without obtaining significant results.

704   We also explored the whole brain using mass univariate tests, knowing that whole brain analyses

705   face the ill-posed problem of correction of multiple comparisons of partly correlated tests, problem

706   not fully solved by the Random Field Theory (Eklund et al., 2016). Moreover, since we performed in

707   total at least nine whole brain searchlight analyses and four whole brain univariate comparisons (T-

708   and F-contrasts for responses to graphemes and colours, see Table S1), we could have set a family-

709   wise error level at 0.05/13. We preferred to keep a non-corrected level for easier comparisons with

710   other studies. The whole brain analyses were used only for exploration, and for every detected

711   cluster we searched for additional evidence (differential response for other comparisons, or

712   correlation with individual differences). Since we did not find any additional evidence, we conclude

713   that these clusters may be false positives. We however mention them (see Table S1) in case

714   additional evidence be found in other studies.

715   For now however, our results further suggest that 3T fMRI studies may not be able yet to identify the

716   neural correlates of the synaesthetic experience of colour (Hupé & Dojat, 2015), probably because

717   those are fine-grained distributed at a resolution lower than our 3-mm^3 voxel resolution, or because

718   the nature of its coding does not translate (well) into BOLD responses. Surprisingly, though, if

719   considering synaesthetic colours simply as a form of mental imagery, we were expecting above-

720   chance decoding performance as observed for other tasks involving mental imagery. Those other

721   tasks, however, typically involved different categories of objects, like food, tools, faces and buildings

722   (Reddy et al., 2010) or objects, scenes, body parts and faces (Cichy, Heinzle, & Haynes, 2012), which

723   evoked stronger BOLD signal in specific areas (like the Fusiform Face Area). Other studies involved

724   retinotopic properties (Thirion et al., 2006) where, again, differences of BOLD signal can be easily

725   observed. Here we were trying to decode mental images within only a single category, colour. This

726   confirms that synaesthetic experiences do not evoke strong BOLD responses, at least when using

727   standard 3T MR scanner, as already suggested by the inconsistency of the published results based on

728   univariate models.

729   Below we consider alternative explanations (e.g., methodological flaws) to the absence in our data of

730   neural traces of the processing of synaesthetic colours.

731   *Colour imagery could not be decoded.*

732   Our study used a protocol very similar to that used by (Bannert & Bartels, 2013), who could decode

733   the typical colour from eight objects, presented as greyscale photos, with classifiers trained on

734   concentric colour circles designed after (Brouwer & Heeger, 2009), like in our study. The prototypical

735   colour of the objects was red, green, blue or yellow (like a banana and a tennis ball). Across 18

736   subjects, decoding accuracy was "significantly" above chance in V1, but reached only 32% on

737   average, which is hardly above the 95% CI ([24 30]%) of the performance observed for our similar

738   classifier ('C2S') in the areas V1 to V4 of synaesthetes. Their experimental procedures, slightly

739   different from ours, may have better optimized the signal to noise ratio and allowed this higher

740   performance (see below). Alternatively, since the colour-diagnostic objects were presented before

741   the coloured concentric rings, subjects may have imagined, when viewing the rings, the very objects

742   that were presented before. Subjects had to do a motion discrimination task to divert their attention

743   (similarly to our one-back task), but such a task (like ours) was not very demanding (though note that

744   Bannert and Bartels argue that their results are due to automatically occurring processes during

745   object vision rather than active imagery). Of course, a similar argument holds even more in our

746   experiment: synaesthetes were very likely to recognize the colour matching exactly their

747   synaesthetic colour of letters and digits, and they might well have imagined the letter or digit when

748   looking at the coloured stimuli. In both cases, decoding would be based on the complex shape of

749   stimuli rather than their colour. In the case of Bannert and Bartels, objects were similar to those used

750   in other successful visual-to-imagery decoding and involved several categories of objects as well as

751   different retinotopic properties (the objects had different orientations but were rotating; however

752   the banana or the coke can, for example, had about 12 deg extent, apparently much more than the

753   Nivea tin or the blue traffic sign), while in our case objects all belonged to the grapheme category,

754   and all spanned the same visual extent. It is therefore possible that in the study by Bannert and

755   Bartels the slightly above chance decoding performance was due to residual category and retinotopic

756   properties, not to colour. With such an interpretation, decoding of imaginary colours would have

757   failed in both their and our study.

758   *Flaw in the paradigm used: duration of event presentation.*

759   Our close to chance performance could be linked to our choice of a fast event related paradigm, each

760   stimulus being presented each time for only 1 s, with an ISI = 1 s +/- 333 ms. Bannert and Bartels

761   presented images for 2 s with a 1 s ISI, each repeated four times in a row (miniblocks). One may

762   wonder whether our presentation time was sufficient to trigger synaesthetic associations. However,

763   psychophysical tasks show that the naming of the synaesthetic colours of graphemes takes on

764   average much less than 1 s (Table 1). Because of our one-back attentional task, though, we cannot be

765   sure that the synaesthetic associations were always conscious. However, synaesthetes did not report

766   any specific difficulty with their synaesthetic experience when viewing, inside the scanner, the

767   proposed paradigm. We designed such a protocol because we did not want synaesthetes to pay too

768   much attention to their synaesthetic colours, then possibly triggering complex attentional and

769   emotional processes. Those components are part of the synaesthetic experience, but they do not tell

770   us anything about the phenomenological experience of colours, our main goal being to try to isolate

771   the possible neural commonalities of the real and synaesthetic experience. The quasi-absence of

772   observed differences of overall activation and modulation between synaesthetes and controls for

773   graphemes indicates that we were successful in synaesthetes having a similar experience to controls

774   for graphemes, in terms of attentional and emotional content. With different conditions, favouring

775   synaesthetic colours to be experienced intensely, we would expect the overall pattern of brain

776   activity to be different, but those differences would be poorly informative.

777   *Flaw in the paradigm used: type of stimuli.*

778   A critical aspect of our fast-event paradigm is related to the slow dynamics of the hemodynamic

779   signal and the signal to noise we could obtain. Here, the critical benchmark was the possibility to

780   decode real colours, since the protocol was identical for synaesthetic and real colours. We were

27

781   successful in decoding colours above chance in the visual cortex, but not to the extent that we

782   hoped: only 35% on average, chance being 25%. Using 12 s miniblocks, Bannert and Bartels obtained

783   an average performance for colours between 35% and 40% in V1 to V4. Differences other than the

784   timing of the stimuli may explain this only slightly higher performance: their total presentation time

785   of coloured stimuli was about 42 min (20 min in our study; for example, Brouwer & Heeger, 2009,

786   obtained even higher performances with experienced participants tested for much longer durations);

787   their stimuli were much larger (7.19 deg *vs.* 2 deg radius) and isoluminant (we do not know whether

788   luminance information in our case helped or hindered decoding). Because they were constrained by

789   the idiosyncratic synaesthetic associations, our stimuli were also not well distributed within the

790   colour space (see Figure 2). Colour differences between categories (R, G, B and Y) and similarity

791   between colours for pairs (letter-digit) were different between subjects and not always optimal to

792   reach maximal performance by classifiers. Probably, some pairs of supposedly similar colours

793   confused classifiers, as well as short distances between some categories. Retrospectively, we should

794   in fact even consider ourselves lucky to have achieved such a performance for colour decoding.

795   Choosing only three colours would have allowed us to avoid confusions and get more exemplars for

796   each colour (with fewer categories to decode, though, confounding factors are more likely). More

797   repetitions would be welcome, however we wanted to record signals for real and synaesthetic

798   colours within the same scanning session to avoid any spatial smoothing of the voxels (which is often

799   necessary when aligning images obtained in different sessions). Preliminary experiments had showed

800   us indeed that combining the signals from different sessions did not improve performance (Ruiz et

801   al., 2012). Our total session time was about 1 hour, which is about the limit one may ask naïve

802   subjects to lie in a scanner without moving while maintaining fixation and attention over boring

803   stimuli.

804   *Lack of statistical power to detect small differences.*

805   Given our moderate performance for colour classification, our absence of above-chance performance

806   for the decoding of synaesthetic colours might be due to a lack of power, since performance across

807   real and imaginary images is typically lower than for real images (Reddy et al., 2010; Bannert &

808   Bartels, 2013). Indeed, if real differences exist between synaesthetes and controls in the measured

809   BOLD signal, these differences are too small to be detected reliably with sample sizes similar to ours,

810   with no indication about the minimum required sample size. Such a reasoning holds for the average

811   performance, but some subjects did reach performance for colour decoding well above 50%. Yet, the

812   distribution of individual scores were all very similar for controls and synaesthetes (see Figs. 5-6).

813   There was some correlation between the performances of colour ('Col') and synaesthetic ('Syn')

814   classifiers in retinotopic areas (especially V1), but it was similar in synaesthetes and controls (the

28

815   differences between synaesthetes and controls for the 'Syn' classifier were in fact even weaker when

816   including the 'Col' performance as a covariate).

817   For the statistical analysis, we adopted the "new statistical approach" proposed by (Cumming, 2012)

818   and focussed on confidence intervals of effect sizes instead of the less informative thresholded p-

819   value maps (Hupé, 2015). In order to facilitate the comparison of our study with previous studies, we

820   indicated when the comparisons could be considered as "significant" (a 95% CI not crossing the

821   chance level corresponds to $p < 0.05$) when correcting the risk level for multiple comparisons. Note

822   however that correction for multiple comparisons corresponds to an ill-posed problem, because

823   there is no unique and objective way to define the family of tests (Hupé, 2015). Such a problem is

824   pretty obvious in our case, where the number of considered ROIs depends on our choice of

825   regrouping or not ROIs, and by how much. We applied a Bonferroni correction over twelve ROIs, but

826   we could have considered the family across the five types of classifiers (so at least 60 tests).

827   However, by focusing on the extent of the CIs, the conclusions do not change much for different

828   levels of CI (the extent of a 99.58% CIs is just a bit larger than for a 95% CI): for all the cases that may

829   suggest differences between groups, the true differences compatible with our observations may be

830   either close to absent (difference close to or including 0, or odds ratio close to or including 1) or at

831   most up to about 15% (or odds ratio = 1.5), a value that one may consider meaningful. As in most

832   studies currently published in cognitive neuroscience dealing with small effects, the width of our

833   confidence intervals is too wide to reach any definitive conclusion on the sole basis of one test (lack

834   of power). Our choice of CI presentation, however, brings useful information allowing cumulative

835   science (Yarkoni, Poldrack, Van Essen, & Wager, 2010) and shows that if any real difference exists, it

836   is probably not very large because corresponding to less than a 15% difference of performance.

837

838   **Conclusion**

839   Identifying the neural correlates of the synaesthetic experience of colours may still be beyond the

840   reach of present technology, including hardware (3T MR scanner) and advanced data analysis

841   techniques such as MVPA, and that we still do not find any evidence of common neural coding of real

842   and synaesthetic colours (Hupé et al., 2012b). However, across all our analyses, we did find several

843   "significant" differences for several comparisons, which we listed in the Results section and detailed

844   in Supporting Information, Table S1. Other studies also did report so-called "significant" effects, even

845   though the methods to determine the significance levels were questionable in most studies (Hupé &

846   Dojat, 2015). We applied the latest recommendations for group-level cluster-wise inferences (9-

847   mmm FWHM spatial smoothing, cluster-defining threshold = 0.001, cluster-based pFWE <0.05,

29

848   groups of 20 participants), yet these criteria do not protect well against false positives (Eklund et al.,

849   2016). In our study, for each "significant" effect, we had a set of independent measures to further

850   explore any difference that may be real: the performance of other classifiers as well as individual

851   differences (the strength of the synaesthetic associations measured in Stoop-like psychophysics

852   tests). We never found any coherence across different measures. Moreover, the locations of the

853   "significant" effects appeared quite randomly across the brain. As long as no other study replicates

854   any of these "differences", we should keep in mind that they could be false positives. Our study thus

855   further shows that common statistical practices based on Null Hypothesis Significance Tests (NHST)

856   are not adequate for scientific inference (Hupé & Dojat, 2015; Wasserstein & Lazar, 2016; Hupé,

857   2017). By stressing that we did not find any evidence of common neural coding of real and

858   synaesthetic colours, based on our data as well as past studies, we do not conclude that such a

859   neural coding does not exist. We bring to light what is required to have any chance to reveal the

860   neural bases of the synaesthetic experience using MRI, like more data by subject, higher signal to

861   noise ratio and spatial resolution (e.g., 7 Tesla scanner: Turner, 2016) and maybe larger cohorts. In

862   order to start contributing to this last aim, via the constitution of dedicated data repositories and

863   meta-analyses, our data are freely available on request (https://shanoir.irisa.fr/Shanoir/login.seam,

864   contact M. Dojat). Please refer to the present paper in case of the reuse of these datasets.

865

866 **References**

867 Bannert, M. M., & Bartels, A. (2013). Decoding the yellow of a gray banana. *Curr. Biol., 23*(22), 2268-
868 2272. doi: 10.1016/j.cub.2013.09.016
869 Bates, D., Mächler, M., Bolker, B., & Walker, S. (2015). Fitting linear mixed-effects models using lme4.
870 *J. Stat. Soft., 67*(1), 48. doi: 10.18637/jss.v067.i01
871 Bordier, C., Hupé, J. M., & Dojat, M. (2015). Quantitative evaluation of fMRI retinotopic maps, from
872 V1 to V4, for cognitive experiments. *Front. Hum. Neurosci., 9*, 277. doi:
873 10.3389/fnhum.2015.00277
874 Brouwer, G. J., & Heeger, D. J. (2009). Decoding and reconstructing color from responses in human
875 visual cortex. *J. Neurosci., 29*(44), 13992-14003. doi: 10.1523/JNEUROSCI.3577-09.2009
876 Caspers, J., Zilles, K., Eickhoff, S. B., Schleicher, A., Mohlberg, H., & Amunts, K. (2013).
877 Cytoarchitectonical analysis and probabilistic mapping of two extrastriate areas of the human
878 posterior fusiform gyrus. *Brain Struct. Funct., 218*(2), 511-526. doi: 10.1007/s00429-012-
879 0411-8
880 Caspers, S., Eickhoff, S. B., Geyer, S., Scheperjans, F., Mohlberg, H., Zilles, K., & Amunts, K. (2008). The
881 human inferior parietal lobule in stereotaxic space. *Brain Struct. Funct., 212*(6), 481-495. doi:
882 10.1007/s00429-008-0195-z
883 Caspers, S., Geyer, S., Schleicher, A., Mohlberg, H., Amunts, K., & Zilles, K. (2006). The human inferior
884 parietal cortex: cytoarchitectonic parcellation and interindividual variability. *NeuroImage,*
885 *33*(2), 430-448. doi: 10.1016/j.neuroimage.2006.06.054
886 Chiou, R., & Rich, A. N. (2014). The role of conceptual knowledge in understanding synaesthesia:
887 Evaluating contemporary findings from a 'hub-and-spoke' perspective. *Front. Psychol., 5*. doi:
888 10.3389/fpsyg.2014.00105
889 Choi, H. J., Zilles, K., Mohlberg, H., Schleicher, A., Fink, G. R., Armstrong, E., & Amunts, K. (2006).
890 Cytoarchitectonic identification and probabilistic mapping of two distinct areas within the
891 anterior ventral bank of the human intraparietal sulcus. *J. Comp. Neurol., 495*(1), 53-69. doi:
892 10.1002/cne.20849
893 Chun, C. A., & Hupé, J. M. (2013). Mirror-touch and ticker tape experiences in synesthesia. *Front.*
894 *Psychol., 4*, 776. doi: 10.3389/fpsyg.2013.00776
895 Chun, C. A., & Hupé, J. M. (2016). Are synesthetes exceptional beyond their synesthetic associations?
896 A systematic comparison of creativity, personality, cognition, and mental imagery in
897 synesthetes and controls. *Brit. J. Psychol., 107*, 397–418. doi: 10.1111/bjop.12146
898 Cichy, R. M., Heinzle, J., & Haynes, J. D. (2012). Imagery and perception share cortical representations
899 of content and location. *Cereb. Cortex, 22*(2), 372-380. doi: 10.1093/cercor/bhr106
900 Cox, D. D., & Savoy, R. L. (2003). Functional magnetic resonance imaging (fMRI) "brain reading":
901 detecting and classifying distributed patterns of fMRI activity in human visual cortex.
902 *NeuroImage, 19*(2 Pt 1), 261-270.
903 Cumming, G. (2012). *Understanding The New Statistics: Effect Sizes, Confidence Intervals, and Meta-*
904 *Analysis*. New York: Routledge.
905 Dehaene, S., & Cohen, L. (2011). The unique role of the visual word form area in reading. *Trends*
906 *Cogn. Sci., 15*(6), 254-262. doi: 10.1016/j.tics.2011.04.003
907 Dojat, M., Pizzagalli, F., & Hupé, J. M. (2018). Magnetic resonance imaging does not reveal structural
908 alterations in the brain of grapheme-color synesthetes. *PLoS ONE, 13*(4), e0194422. doi:
909 10.1371/journal.pone.0194422
910 Eagleman, D. M., Kagan, A. D., Nelson, S. S., Sagaram, D., & Sarma, A. K. (2007). A standardized test
911 battery for the study of synesthesia. *J. Neurosci. Methods, 159*(1), 139-145. doi:
912 10.1016/j.jneumeth.2006.07.012
913 Edquist, J., Rich, A. N., Brinkman, C., & Mattingley, J. B. (2006). Do synaesthetic colours act as unique
914 features in visual search? *Cortex, 42*(2), 222-231.

915 Eickhoff, S. B., Paus, T., Caspers, S., Grosbras, M. H., Evans, A. C., Zilles, K., & Amunts, K. (2007).
916   Assignment of functional activations to probabilistic cytoarchitectonic areas revisited.
917   *NeuroImage, 36*(3), 511-521. doi: 10.1016/j.neuroimage.2007.03.060
918 Eklund, A., Nichols, T. E., & Knutsson, H. (2016). Cluster failure: Why fMRI inferences for spatial
919   extent have inflated false-positive rates. *Proc. Natl. Acad. Sci. USA, 113*(28), 7900-7905. doi:
920   10.1073/pnas.1602413113
921 Flournoy, T. (1893). *Des Phénomènes de Synopsie (Audition Colorée): Photismes, Schèmes Visuels,*
922   *Personnifications.* Paris: Alcan.
923 Formisano, E., & Kriegeskorte, N. (2012). Seeing patterns through the hemodynamic veil--the future
924   of pattern-information fMRI. *NeuroImage, 62*(2), 1249-1256. doi:
925   10.1016/j.neuroimage.2012.02.078
926 Galton, F. (1880). Statistics of mental imagery. *Mind, 5*, 301-318.
927 Gebuis, T., Nijboer, T. C., & Van der Smagt, M. J. (2009). Multiple dimensions in bi-directional
928   synesthesia. *Eur. J. Neurosci., 29*(8), 1703-1710. doi: 10.1111/j.1460-9568.2009.06699.x.
929 Grill-Spector, K., Kourtzi, Z., & Kanwisher, N. (2001). The lateral occipital complex and its role in
930   object recognition. *Vision Res., 41*(10-11), 1409-1422. doi: 10.1016/S0042-6989(01)00073-6
931 Hebart, M. N., & Baker, C. I. (2017). Deconstructing multivariate decoding for the study of brain
932   function. *NeuroImage.* doi: 10.1016/j.neuroimage.2017.08.005
933 Hupé, J. M. (2015). Statistical inferences under the Null hypothesis: Common mistakes and pitfalls in
934   neuroimaging studies. *Front. Neurosci., 9*, 18. doi: 10.3389/fnins.2015.00018
935 Hupé, J. M. (2017). Comment on "Ducklings imprint on the relational concept of 'same or different'".
936   *Science, 355*(6327), 806-806. doi: 10.1126/science.aah6047
937 Hupé, J. M., Bordier, C., & Dojat, M. (2012a). A BOLD signature of eyeblinks in the visual cortex.
938   *NeuroImage, 61*, 149–161. doi: 10.1016/j.neuroimage.2012.03.001
939 Hupé, J. M., Bordier, C., & Dojat, M. (2012b). The neural bases of grapheme-color synesthesia are not
940   localized in real color sensitive areas. *Cereb. Cortex, 22*, 1622:1633. doi:
941   10.1093/cercor/bhr236
942 Hupé, J. M., & Dojat, M. (2015). A critical review of the neuroimaging literature on synesthesia. *Front.*
943   *Hum. Neurosci., 9*, 103. doi: 10.3389/fnhum.2015.00103
944 Janik McErlean, A. B., & Banissy, M. J. (2017). Color processing in synesthesia: what synesthesia can
945   and cannot tell us about mechanisms of color processing. *Top. Cogn. Sci., 9*(1), 215-227. doi:
946   10.1111/tops.12237
947 Kriegeskorte, N., Goebel, R., & Bandettini, P. (2006). Information-based functional brain mapping.
948   *Proc. Natl. Acad. Sci. USA, 103*(10), 3863-3868. doi: 10.1073/pnas.0600244103
949 Lorenz, S., Weiner, K. S., Caspers, J., Mohlberg, H., Schleicher, A., Bludau, S., . . . Amunts, K. (2017).
950   Two new cytoarchitectonic areas on the human mid-fusiform gyrus. *Cereb. Cortex, 27*(1),
951   373-385. doi: 10.1093/cercor/bhv225
952 Mumford, J. A., Turner, B. O., Ashby, F. G., & Poldrack, R. A. (2012). Deconvolving BOLD activation in
953   event-related designs for multivoxel pattern classification analyses. *NeuroImage, 59*(3),
954   2636-2643. doi: 10.1016/j.neuroimage.2011.08.076
955 Norman, K. A., Polyn, S. M., Detre, G. J., & Haxby, J. V. (2006). Beyond mind-reading: multi-voxel
956   pattern analysis of fMRI data. *Trends Cogn. Sci., 10*(9), 424-430. doi:
957   10.1016/j.tics.2006.07.005
958 Parkes, L. M., Marsman, J. B., Oxley, D. C., Goulermas, J. Y., & Wuerger, S. M. (2009). Multivoxel fMRI
959   analysis of color tuning in human primary visual cortex. *J. Vis., 9*(1), 1 1-13. doi: 10.1167/9.1.1
960 Pedregosa, F., Varoquaux, G., Gramfort, A., Michel, V., Thirion, B., Grisel, O., . . . Duchesnay, E.
961   (2011). Scikit-learn: Machine Learning in Python. *J. Mach. Learn. Res., 12*, 2825-2830.
962 Poldrack, R. A. (2007). Region of interest analysis for fMRI. *Soc. Cogn. Affect. Neurosci., 2*(1), 67-70.
963   doi: 10.1093/scan/nsm006
964 Reddy, L., Tsuchiya, N., & Serre, T. (2010). Reading the mind's eye: decoding category information
965   during mental imagery. *NeuroImage, 50*(2), 818-825. doi: 10.1016/j.neuroimage.2009.11.084

966 Reeder, R. R. (2016). Individual differences shape the content of visual representations. *Vision Res.*
967   doi: 10.1016/j.visres.2016.08.008
968 Rouw, R., & Scholte, H. S. (2010). Neural basis of individual differences in synesthetic experiences. *J.*
969   *Neurosci., 30*(18), 6205-6213. doi: 10.1523/JNEUROSCI.3444-09.2010
970 Rouw, R., & Scholte, H. S. (2016). Personality and cognitive profiles of a general synesthetic trait.
971   *Neuropsychologia, 88*, 35-48. doi: 10.1016/j.neuropsychologia.2016.01.006
972 Ruiz, M. J., & Hupé, J. M. (2015). Assessment of the hemispheric lateralization of grapheme-color
973   synesthesia with Stroop-type tests. *PLoS ONE, 10*(3), e0119377. doi:
974   10.1371/journal.pone.0119377
975 Ruiz, M. J., Hupé, J. M., & Dojat, M. (2012). *Use of pattern-information analysis in vision science: a*
976   *pragmatic examination.* Paper presented at the MLMI, Nice.
977 Scheperjans, F., Hermann, K., Eickhoff, S. B., Amunts, K., Schleicher, A., & Zilles, K. (2008). Observer-
978   independent cytoarchitectonic mapping of the human superior parietal cortex. *Cereb. Cortex,*
979   *18*(4), 846-867. doi: 10.1093/cercor/bhm116
980 Simner, J., & Carmichael, D. A. (2015). Is synaesthesia a dominantly female trait? *Cogn. Neurosci.,*
981   *6*(2-3), 68-76. doi: 10.1080/17588928.2015.1019441
982 Simner, J., Mulvenna, C., Sagiv, N., Tsakanikos, E., Witherby, S. A., Fraser, C., . . . Ward, J. (2006).
983   Synaesthesia: The prevalence of atypical cross-modal experiences. *Perception, 35*(8), 1024-
984   1033. doi: 10.1068/p5469
985 Stelzer, J., Lohmann, G., Mueller, K., Buschmann, T., & Turner, R. (2014). Deficient approaches to
986   human neuroimaging. *Front. Hum. Neurosci., 8*(462). doi: 10.3389/fnhum.2014.00462
987 Thirion, B., Duchesnay, E., Hubbard, E., Dubois, J., Poline, J. B., Lebihan, D., & Dehaene, S. (2006).
988   Inverse retinotopy: inferring the visual content of images from brain activation patterns.
989   *NeuroImage, 33*(4), 1104-1116. doi: 10.1016/j.neuroimage.2006.06.062
990 Tootell, R. B. H., & Nasr, S. (2017). Columnar segregation of magnocellular and parvocellular streams
991   in human extrastriate cortex. *J. Neurosci., 37*(33), 8014-8032. doi: 10.1523/jneurosci.0690-
992   17.2017
993 Turner, R. (2016). Uses, misuses, new uses and fundamental limitations of magnetic resonance
994   imaging in cognitive science. *Philos. Trans. R. Soc. Lond. B. Biol. Sci., 371*(1705). doi:
995   10.1098/rstb.2015.0349
996 Vasseur, F., Delon-Martin, C., Bordier, C., Warnking, J., Lamalle, L., Segebarth, C., & Dojat, M. (2010).
997   fMRI retinotopic mapping at 3 T: Benefits gained from correcting the spatial distortions due
998   to static field inhomogeneity. *J. Vis., 10 (12)*, 30. doi: 10.1167/10.12.30
999 Ward, J. (2013). Synesthesia. *Annual Reviews in Psychology, 64*, 49–75. doi: 10.1146/annurev-psych-
1000   113011-143840
1001 Wasserstein, R. L., & Lazar, N. A. (2016). The ASA's Statement on p-Values: Context, Process, and
1002   Purpose. *The American Statistician, 70*(2), 129-133. doi: 10.1080/00031305.2016.1154108
1003 Watson, M. R., Chromy, J., Crawford, L., Eagleman, D. M., Enns, J. T., & Akins, K. A. (2017). The
1004   prevalence of synaesthesia depends on early language learning. *Conscious Cogn., 48*, 212-
1005   231. doi: 10.1016/j.concog.2016.12.004
1006 Witthoft, N., & Winawer, J. (2013). Learning, memory, and synesthesia. *Psychol. Sci., 24*(3), 258-265.
1007   doi: 10.1177/0956797612452573
1008 Yarkoni, T., Poldrack, R. A., Van Essen, D. C., & Wager, T. D. (2010). Cognitive neuroscience 2.0:
1009   building a cumulative science of human brain function. *Trends Cogn. Sci., 14*(11), 489-496.
1010   doi: 10.1016/j.tics.2010.08.004
1011
1012

1013 **Appendix**

1014 **Supporting Information** is available. It contains:

1015 Table S1. Clusters identified based on whole brain analyses and tested *post-hoc* with MVPA.

1016 Figure S1. Right occipito-parietal cortex cluster identified based on whole brain univariate analysis

1017 Figure S2. Left anterior insula cluster identified based on whole brain univariate analysis

1018 Figure S3. Right frontal cortex cluster identified based on whole brain univariate analysis

1019 Figure S4. Alternative version of Figure 5, based on mixed-effect generalized linear models

1020 Figure S5. Alternative version of Figure 6, based on mixed-effect generalized linear models

1021

1022

1023 **Author Contributions**

1024 M.J.R., M.D, and J.-M.H. designed research; M.J.R. and M.D. performed research; M.J.R., M.D, and J.-

1025 M.H. analysed data; J.-M.H. wrote the paper; M.J.R., M.D, and J.-M.H. revised the paper.

1026

1027 **Competing Interests**

1028 The authors declare no competing interests, financial or non-financial.